Enzyme-Free Sugar Sensing in Microfluidic Channels with an Affinity-Based Single-Wall Carbon Nanotube Sensor

Alexis Vlandas,[†] Tetiana Kurkina,[†] Ashraf Ahmad,[†] Klaus Kern,[†,‡] and Kannan Balasubramanian*,[†]

Max-Planck-Institute for Solid State Research, Heisenbergstrasse 1, D-70569, Stuttgart, Germany and Institut de Physique de la Matière Condensée, Ecole Polytechnique Fédérale de Lausanne, CH-1015 Lausanne, Switzerland

We present a novel nonenzymatic carbon nanotube sensor integrated in a microfluidic channel for the detection of sugars. The sensor is assembled as a liquid-gated field-effect transistor, with the transistor channel composed of 1 to 10 nanotubes, which are controllably functionalized with boronic acid receptors. The devices show sensitivity to glucose in a concentration range of 5 to 30 mM. Furthermore, by controlling the type of nanotube-receptor coupling (as covalent or noncovalent) and by deploying a sensitive impedance-based detection technique, we corroborate in detail the transduction mechanism of our affinity-based sensor. In the case of covalent coupling, charge carrier scattering along the nanotubes is the dominant mechanism. While in the noncovalent case, surface charge effects dominate. The identification of the mechanism along with the tunability of the chemical coupling and the cost-effective integration in microchannels constitute a solid basis for the entry of nanotube-based sensors in lab-on-a-chip applications.

Carbohydrates are important markers for different diseases, the most common of them being glucose for diabetes.[1] Glucose sensors mostly rely on the use of an enzyme such as glucose oxidase (GOx) or glucose dehydrogenase to generate redox mediator species, which are thereafter detected electrochemically.[2] These sensors require the coupling of the enzyme in close proximity to the transducing electrode to obtain high sensitivity. Carbon nanotubes (CNTs) in the form of a film or paste electrode have been employed as electrode material due to their nanoscale size and high electrochemical activity.[3] While providing good selectivity to glucose, such sensors rely on the rate of reaction between the enzyme and glucose and hence are inherently sensitive to factors influencing enzyme activity.[4] In addition, the limited stability of the immobilized enzyme may restrict the shelf life of such sensor systems and their application in in vivo glucose monitoring.[5] Apart from electrochemical transduction, field-effect based detection has also been presented using a CNT-GOx sensor.[6] However, the sensing mechanism and concentration dependence were not discussed there.

During the past decade, there has been a tremendous amount of research directed toward the realization of nonenzymatic glucose sensors.[7] One major approach involves the direct oxidation of glucose at nanostructured electrodes.[8–10] The nanostructuring allows the detection of glucose at a lower overpotential.[7,11] However, such electrodes are very sensitive to adsorbed interferents such as the amount of chloride and suffer from surface fouling over longer times.[12,13] An alternative enzymeless approach for glucose detection involves the use of fully synthetic receptors, such as boronic acid (BA) containing compounds. BA binds reversibly with *cis*-1,2- and *cis*-1,3-diols to form five- and six-membered cyclic esters, respectively.[14,15] On the basis of this, fluorescence sensors,[16,17] potentiometric/amperometric sensors,[18,19] and recently, a field-effect based sensor[20] have been demonstrated. The chemical structure of the boronic acid receptor can be optimized to obtain highly selective and sensitive affinity-based glucose sensors.[16] In addition to glucose, free carbohydrates, as well as their conjugates, such as liposaccharides and glycoproteins

---

* To whom correspondence should be addressed. E-mail: b.kannan@fkf.mpg.de.

† Max-Planck-Institute for Solid State Research.

‡ Institut de Physique de la Matière Condensée, Ecole Polytechnique Fédérale de Lausanne.

(1) Kernohan, A. F. B.; Perry, C. G.; Small, M. *Clin. Chem. Lab. Med.* **2003**, *41*, 1239–1245.
(2) Wang, J. *J. Chem. Rev.* **2008**, *108*, 814–825.
(3) Balasubramanian, K.; Burghad, M. *Anal. Bioanal. Chem.* **2006**, *385*, 452–468.
(4) Gough, D. A.; Leypoldt, J. K.; Armour, J. C. *Diabetes Care* **1982**, *5*, 190–198.
(5) Wilson, G. S.; Gifford, R. *Biosens. Bioelectron.* **2005**, *20*, 2388–2403.
(6) Besteman, K.; Lee, J.; Wiertz, F. G. M.; Heering, H. A.; Dekker, C. *Nano Lett.* **2003**, *3*, 727–730.
(7) Park, S.; Boo, H.; Chung, T. D. *Anal. Chim. Acta* **2006**, *556*, 46–57.
(8) Yuan, J.; Wang, K.; Xia, X. *Adv. Funct. Mater.* **2005**, *15*, 803–809.
(9) Cherevko, S.; Chung, C.-H. *Sens. Actuat. B* **2009**, *142*, 216–223.
(10) Wang, G.; Wei, Y.; Zhang, W.; Zhang, X.; Fang, B.; Wang, L. *Microchim. Acta* **2010**, *168*, 87–92.
(11) Ozcan, L.; Sahin, Y.; Tuerk, H. *Biosens. Bioelectron.* **2008**, *24*, 512–517.
(12) Satheesh Babu, T. G.; Ramachandran, T. *Electrochim. Acta* **2010**, *55*, 1612–1618.
(13) Vassiliyev, Y. B.; Khazova, O. A.; Nikolaeva, N. N. *J. Electroanal. Chem.* **1985**, *196*, 105–125.
(14) James, T. D.; Phillips, M. D.; Shinkai, S. *Boronic Acids in Saccharide Recognition*; RSC Publishing: London, 2006.
(15) Lorand, J. P.; Edwards, J. O. *J. Org. Chem.* **1959**, *24*, 769–774.
(16) Fang, H.; Kaur, G.; Wang, B. *J. Fluoresc.* **2004**, *14*, 481–489.
(17) Pickup, J. C.; Hussain, F.; Evans, N. D.; Rolinski, O. J.; Birch, D. J. S. *Biosens. Bioelectron.* **2005**, *20*, 2555–2565.
(18) Arimori, S.; Ushiroda, S.; Peter, L. M.; Jenkins, A. T. A.; James, T. D. *Chem. Commun.* **2002**, 2368–2369.
(19) Shoji, E.; Freund, M. S. *J. Am. Chem. Soc.* **2001**, *123*, 3383–3384.
(20) Matsumoto, A.; Sato, N.; Sakata, T.; Kataoka, K.; Miyahara, Y. *J. Solid State Electrochem.* **2009**, *13*, 165–170.

are also important in the diagnosis of pathological states, such as cancer.[21,22] While enzyme-based sensors are not directly amenable for the detection of bound sugars, an affinity-based sensor can potentially be deployed for the detection of both free and bound sugars.[22–24] In contrast to enzymatic sensors, the detection principle here is based on complexation, which is a reversible, equilibrium-based reaction without the consumption of the analyte.

Here, we demonstrate an electrical sensor for sugars based on CNTs functionalized with a boronic acid receptor. To our knowledge, this is a unique realization of a CNT sugar sensor, which does not rely on enzymes or electrochemical redox mediators to function, but rather on a combination of affinity sensing and the field effect transistor (FET) effect. The various mechanisms underpinning the detection of glucose are therefore investigated and discussed in detail. Our key strategy comprises the ability to control the kind of chemical coupling (covalent or noncovalent) between the boronic acid receptor and the nanotube. For this purpose, we utilize an electrochemical functionalization route that we have developed to fabricate carbon nanotube[25,26] and graphene[27] sensors. Furthermore, the sensor is fabricated using a strategy that enables the use of both metallic and semiconducting nanotubes.[25,28] The sensor trials are performed in microfluidic channels, allowing for the future integration of several such sensors, each targeting a different analyte. Furthermore, the sensor can be integrated with other processing elements, such as actuators, pumps, etc. on a chip. This will enable the direct processing of physiological fluids such as blood closer to the patient leading to a faster diagnosis of diseases. This platform aspect is an important step toward lab-on-a-chip applications for, e.g., point-of-care diagnostics.[29] While the present sensor is not selective to a single type of sugar, this can be overcome by the use of boronic acid receptors appropriate for a desired carbohydrate.[30,31]

EXPERIMENTAL SECTION

Single wall carbon nanotubes (SWCNTs) (purified HiPco, Unidym Inc.) were dispersed by sonication in 0.1% Triton-X-100. Nondispersed material was removed using filtration followed by centrifugation for 30 min at 15 000 $\times g$. Using standard photolithography, 100-nm thick Pt electrodes with a 2.5 μm gap were prepared on 4 in. Si/SiO$_2$ wafers, which were subsequently cut in 30 $\times$6 mm samples, each containing two device positions.

Thereafter, SWCNTs were dielectrophoretically trapped across the electrode gaps using a signal generator (Agilent 33250A, 10 MHz, 10 V, 15 s). This strategy is advantageous since it is possible to obtain aligned nanotubes of controlled density at desired locations on the chip. We use a standard procedure for preparing the nanotube dispersion, which ensures that we have a similar distribution of nanotubes during every trapping step.[32,33] After dielectrophoresis, the samples were thoroughly washed with acetone and isopropanol and dried in nitrogen flow. The samples were then heated for 2 h at 250 °C to remove the surfactant molecules from the nanotube surface. In order to avoid measurement artifacts arising from electrodes in contact with the solution, the electrodes were covered with a 200 nm SiO$_2$ passivation layer[34] and annealed in argon at 600 °C for 45 s. The resulting nanotube devices were characterized using an Atomic Force Microscope (Digital Instruments Dimension III, see Figure 1(a)) and impedance spectroscopy (Agilent 33250A).

For the fabrication of the microfluidic channel, polydimethylsiloxane (PDMS: Sylgard 184, 10:1 ratio) was used to prepare 2-mm thick plates with a 30-μm channel. The degassed mixture was poured on a SU-8 mold and baked at 65 °C for 1 h. The sample is then placed on a chip carrier and covered with PDMS and glass plates, so that the nanotube devices were integrated into the microchannel (see Figure 1(b),(c)). The flow of the solutions was regulated using a computerized pressure-based flow control system (MFCS-4C, Fluigent). An Ag/AgCl reference electrode placed in contact with the liquid in the microfluidic circuit allows us to set the potential precisely on the surface of the nanotube. This electrode serves two purposes namely as a reference electrode for electrochemical functionalization and as a gate electrode for measuring the FET characteristics.[28]

The sensing trials were performed on more than 10 devices using varying concentrations of glucose solutions in 10 mM phosphate buffer (pH 8.4). The impedance (Z, a complex quantity with magnitude and phase) constitutes the sensor response, which was measured using an impedance analyzer (Agilent 33250A LCR Meter) in a frequency range of 20 Hz to 2 MHz. Using an AC signal to record the sensor characteristics improves the signal-to-noise ratio and reproducibility compared to a DC measurement while enabling acquisition of both the magnitude and phase spectra of the sensor. This frequency response is measured at varying gate voltages to characterize the field-effect behavior. The gate voltages are maintained in the range of −0.4 to 0.2 V (at the Ag/AgCl reference) to ensure that no direct electrochemical oxidation of glucose can take place.[35] The resulting data set can be visualized in the form of a magnitude map as shown in Figure 2. The X-axis corresponds to the liquid gate voltage, while the Y-axis indicates frequency. Every point in the image corresponds to the magnitude of impedance at a certain frequency and gate voltage. These 2D Z-maps contain the complete electrical characteristics of the sensor and can be used to probe in detail their transduction mechanism.

(21) Liu, S.; Miller, B.; Chen, A. *Electrochem. Commun.* **2005**, *7*, 1232–1236.
(22) Song, S. Y.; Yoon, H. C. *Sens. Actuators B* **2009**, *140*, 233–239.
(23) Aime, S.; Botta, M.; Dastru, W.; Fasano, M.; Panero, M.; Arnelli, A. *Inorg. Chem.* **1993**, *32*, 2068–2071.
(24) Djanashvili, K.; Frullano, L.; Peters, J. A. *Chem.—Eur. J.* **2005**, *11*, 4010–4018.
(25) Maroto, A.; Balasubramanian, K.; Burghad, M.; Kern, K. *ChemPhysChem* **2007**, *8*, 220–223.
(26) Schlecht, U.; Balasubramanian, K.; Burghard, M.; Kern, K. *Appl. Surf. Sci.* **2007**, *253*, 8394–8397.
(27) Sundaram, R. S.; Gomez-Navarro, C.; Balasubramanian, K.; Burghard, M.; Kern, K. *Adv. Mater.* **2008**, *20*, 3050–3053.
(28) Balasubramanian, K.; Burghad, M.; Kern, K. *Phys. Chem. Chem. Phys.* **2008**, *10*, 2256–2262.
(29) Oosterbroek,E.; van den BergA. *Miniaturized Systems for Biochemical Analysis and Synthesis*; Elsevier: New York, 2003.
(30) Karnati, V. V.; Gao, X.; Gao, S.; Yang, W.; Ni, W.; Sankar, S.; Wang, B. *Bioorg. Med. Chm. Lett.* **2002**, *12*, 3373–3377.
(31) Chimpuku, C.; Ozawa, R.; Sasaki, A.; Sato, F.; Hashimoto, T.; Yamauchi, A.; Suzuki, I.; Hayashita, T. *Chem. Commun.* **2009**, *13*, 1709–1712.
(32) Ahmad, A.; Kern, K.; Balasubramanian, K. *ChemPhysChem* **2009**, *10*, 905–909.
(33) Ahmad, A.; Kurkina, T.; Kern, K.; Balasubramanian, K. *ChemPhysChem* **2009**, *10*, 2251–2255.
(34) Sagar, A. S.; Kern, K.; Balasubramanian, K. *Nanotechnology* **2010**, *21*, 015303.
(35) Park, S.; Boo, H.; Chung, T. D. *Anal. Chim. Acta* **2006**, *556*, 46–57.

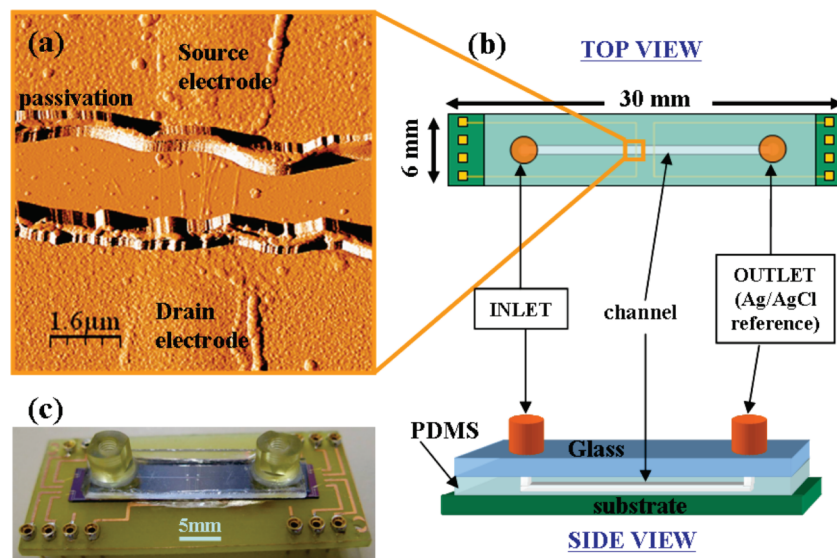**Figure 1.** (a) An Atomic Force Microscope (AFM) image of the electrode region of a BA-CNT sensor after the sensing trials The SiO_2 passivation layer can be seen extending above both electrodes. (b) A schematic representation of the microfluidic set up with the location of the nanotube device. The channel is carved out in the PDMS layer and the nanotube device is directly below the channel on the substrate. (c) A photograph of the final assembled device. The Ag/AgCl reference that acts as a gate electrode is placed in the waste reservoir that is connected to the outlet.
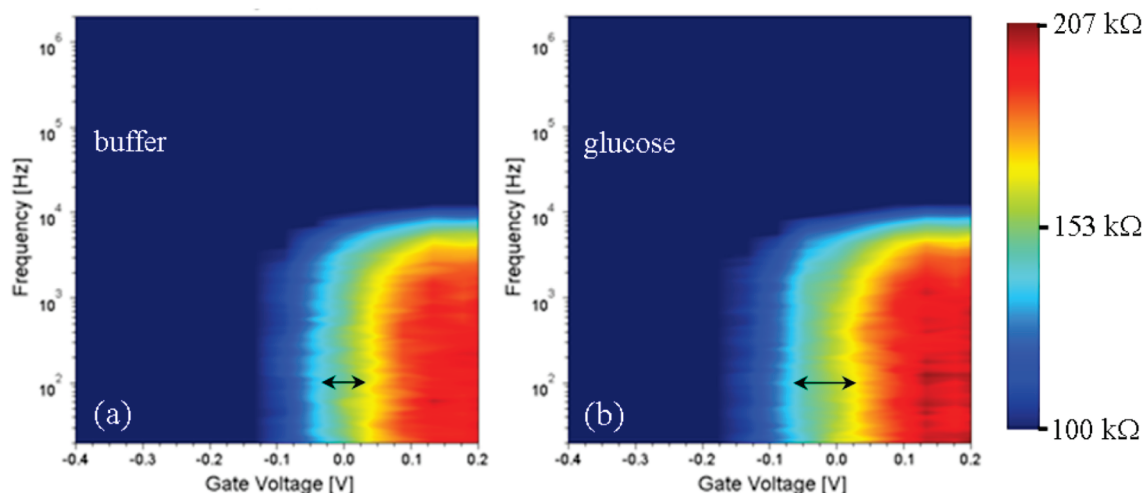

Figure 2. 2D impedance (Z-) maps showing the impedance as a function of frequency and liquid gate voltage. Magnitude [Ohms] maps of the impedance of covalently functionalized BA-CNT devices are shown in buffer (a) and in 10 mM glucose (b). Subtle changes in the impedance response can be clearly seen upon exposure of the sensor to glucose as indicated by the twin-headed black arrows.

RESULTS AND DISCUSSION

The BA receptors were coupled to the surface of the trapped carbon nanotubes through electrochemical functionalization. This method is well established as a versatile route to obtain covalent or noncovalent moieties on the nanotube surface.[36] 3-Aminophenylboronic acid is used as the precursor and the functionalization is carried out directly in the microchannel according to Scheme 1. In order to covalently attach the phenylboronic acid receptor to the nanotube, a highly reactive diazonium radical is created, which binds to the tube via reductive coupling. For this purpose, the microchannel is filled with the diazonium solution and the voltage at the nanotube scanned between +0.1 and −0.55 V versus Ag/AgCl. The formation of the covalent bond is confirmed by the continuous increase in resistance during the sweep[28] and

subsequently by Raman spectra[37] (see Supporting Information, Figure S1). Noncovalent attachment is achieved via direct electro polymerization of the amine under oxidative conditions,[37] by sweeping the voltage at the nanotube from −0.1 V to +0.55 V versus Ag/AgCl for a fixed time period. The resistance in this case increases only slightly during the sweep. After functionalization, 10 mM H_2SO_4 and water are flushed through the microchannel. The diameter of the tubes barely increases in the covalent case, while the noncovalent coupling results in a height increase of 1 to 3 nm, as inferred from AFM measurements. On the basis of these observations and data from available reports,[38−40] we conclude that the number of BA moieties attached in the covalent case are just a few and are
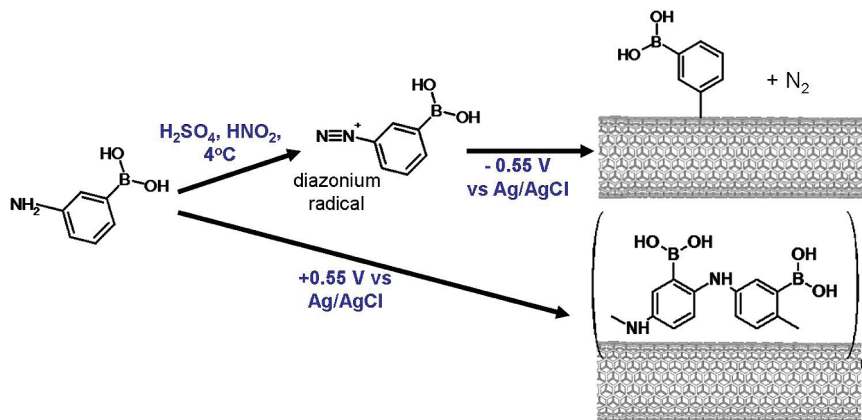
(36) Balasubramanian, K.; Burghard, M. *J. Mater. Chem.* **2008**, *18*, 3071–3083.

(37) Balasubramanian, K.; Friedrich, M.; Jiang, C.; Fan, Y.; Mews, A.; Burghard, M.; Kern, K. *Adv. Mater.* **2003**, *15*, 1515–1518.
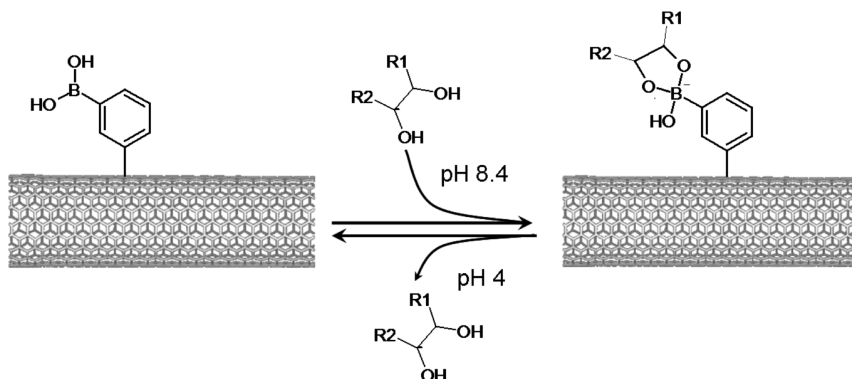(38) Bahr, J. L.; Tour, J. M. *J. Mater. Chem.* **2002**, *12*, 1952–1958.
(39) Downard, A. J. *Electroanalysis* **2000**, *12*, 1085–1096.

Scheme 1. Functionalization Strategy to Obtain the BA-CNT-Sensors[a]

[a] For covalent attachment (top route), the phenyl boronic acid precursor is converted into a reactive diazonium radical through diazotization at 4°C. This cold solution is flushed through the microchannel and the electrochemical functionalization of the nanotube carried out under reductive conditions (-0.55 V vs. Ag/AgCl). To obtain a non-covalent attachment (bottom route), the precursor is directly electropolymerized to obtain a polymer wrapping on the nanotube surface under oxidative conditions at room temperature.

Scheme 2. Affinity Sensing of Glucose: Binding of Glucose to Boronic Acid-Functionalized Carbon Nanotube[a]

[a] The formation of the ester leads to an increase in relative negative charge at the surface of the nanotube which can be detected electrically. The reaction is reversible at low pH. In an acid solution at a pH of ∼4, the attached sugar can be released going back to the initial state.

sparsely distributed on the nanotube surface. On the contrary, in the noncovalent case we have a large number of BA moieties that present a near-to-complete coverage of the CNT surface.

We will first focus our discussion on the sensing response of the covalently coupled BA-CNT devices. The general idea behind the functioning of the sensor is shown in Scheme 2. The binding of glucose to the attached BA *receptors* leads to a change in the net charge distribution on the nanotube surface, which can be sensed through changes in the impedance of the nanotube (see later discussion for a detailed picture). The *Z*-maps of a typical sensor in buffer and in glucose are shown in Figure 2(a),(b), respectively. The magnitude plots show subtle differences in the low frequency region. These variations are further apparent in the cross-section profiles collected in Figure 3(a),(b). These section profiles are extracted from the *2D Z*-maps by plotting either the frequency response at a fixed gate voltage (Figure 3(a)) or the gate dependence at specific frequencies (Figure 3(b)). From the magnitude spectrum in Figure 3(a), it is apparent that at low frequencies, the device acts as a resistor, while capacitive effects become dominant as the frequency increases. The resistance of the device shows nominally a 5% increase upon binding of glucose,

as is apparent in Figure 3(a). The increase in resistance can be attributed to stronger scattering centers due to the increase in net charge when glucose binds to the receptor sites on the nanotube (see Scheme 2). This mechanism is consistent with the occurrence of analyte dependent carrier scattering, as we have demonstrated for covalently functionalized CNT-based pH sensors.[25] Further support for the scattering based sensor response is obtained from the gate voltage dependence in Figure 3(b), where it is apparent that the higher resistance persists over almost the entire gate voltage range. The response to glucose is reversible as discussed in the Supporting Information section (Figure S2). Control experiments performed with CNTs that were not functionalized did not show any significant changes up to a concentration of 20 mM glucose (Figure S3, Supporting Information). We have obtained similar results also with fructose (see Figure S4 in Supporting Information).

Now, we turn toward the concentration response of the covalently functionalized BA-CNT sensors. Toward this purpose, the devices were exposed to successive aliquots of a 5 mM glucose solution. A 1-μL aliquot of the analyte solution was flushed over the sensor at a precise speed, followed by 9 μL of buffer solution at which point the flow was stopped and the impedance measured. This cycle was repeated several times. The *Z*-maps for the various
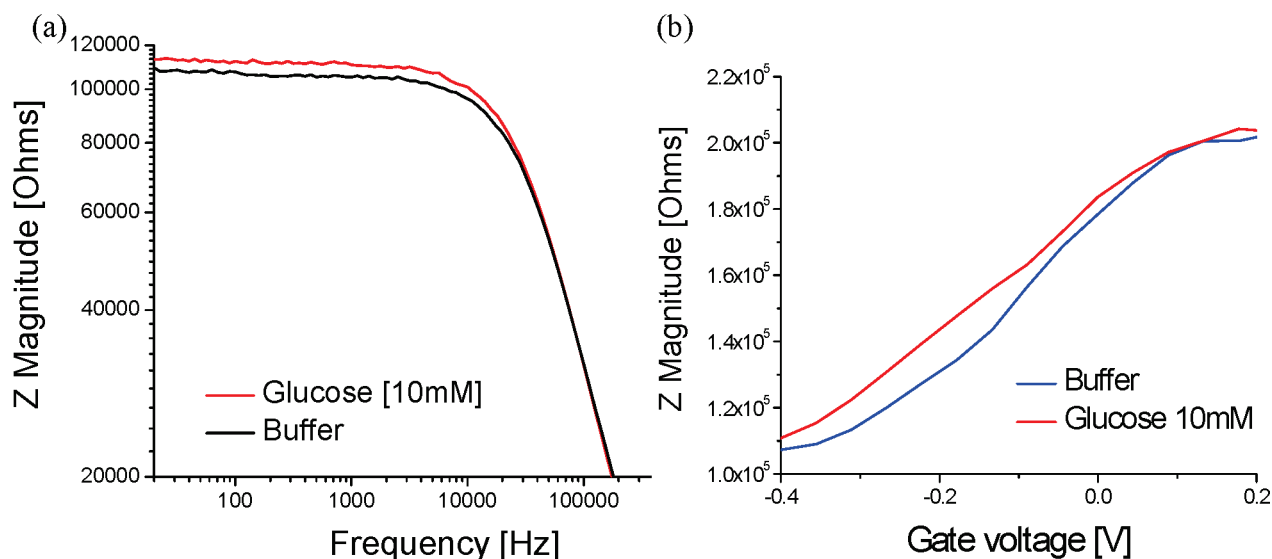
(40) Balasubramanian, K.; Burghard, M. *Small* **2005**, *2*, 180–192.

Figure 3. Frequency response profiles extracted from the *2D Z*-maps shown in Figure 2. (a) Magnitude of impedance of the covalent-BA-CNT sensor as a function of frequency at a fixed gate voltage of −0.4 V, showing the sensor response upon introduction of glucose. The magnitude of impedance at low frequencies increases by around 5% in the presence of 10 mM glucose. (b) Liquid gate dependence of the magnitude of impedance of the covalent-BA-CNT sensor at low frequencies (20−200 Hz) extracted from the *2D Z*-map in Figure 2. The impedance increases in almost the entire gate voltage range upon exposure to glucose.

injections are collected in Figure 4(a). It is apparent that with every injection the response to glucose becomes stronger. This is further clarified in the line profiles in Figure 4(b), which show the relative increase in the magnitude of impedance for various injections. The calibration plot shown in figure 4(c) displays a clear trend of the sensor signal as a function of glucose exposure. It can be seen that with every exposure, the sensor signal increases, however it tends to saturate for larger injections. This behavior is expected due to the finite number of BA moieties that can complex with the incoming glucose molecules. It is noteworthy that by using this multiple injection procedure, one can adjust the volume flushed through the channel to operate the sensor in a desired concentration range.

An initial idea about the performance of the realized sensor can be obtained from the data summarized in Table 1 (see also Figure S5 in Supporting Information, showing real-time data). On the basis of this initial proof-of-concept presented here, there is scope for optimizing the sensor parameters to improve performance. Although there is no exactly parallel enzymatic system similar to the one reported here, it is worth comparing this sensor with well-established enzymatic approaches. The sensitivity of our system is still inferior to typical enzymatic sensors.[3] However, the sensor is stable for up to two weeks. If we were to use enzymes, then there would be very few molecules of the enzyme that would be immobilized on the nanotube surface (keeping in mind that the average number of tubes in our devices is around 5). It would be quite difficult to have the few enzymes in their active state for more than a couple of sensor trials. Furthermore, the enzymatic sensors work on the principle of electrochemical oxidation and hence are prone to common interferents such as acetaminophen, ascorbic acid, and uric acid.[41,42] For our sensors, we have observed that such interferents do not cause a considerable sensor response

(see Figure S6 in Supporting Information for the case of acetaminophen). This is expected since the BA moieties exhibit a high degree of selectivity to sugars.[42]

Sensor Mechanism. In order to elucidate the sensing mechanism, we take a closer look at the physicochemical phenomena responsible for the impedance changes brought by exposure to glucose. For this purpose, the reversible binding of boronic acid to sugars on the surface of CNTs must first be presented. A schematic of this equilibrium can be seen in Figure 5. In the absence of glucose, the neutral (**1**) and negatively charged (**2**) forms of the attached phenyl boronic acid exist in equilibrium with a certain pK_a ($pK_{a1} \approx 8.8$).[43] *cis*-1,2- and *cis*-1,3-diols complex with boronic acid at high pH (>5.8) to form cyclic esters. The complexed forms (**3** and **4**) have a pK_a ($pK_{a2} \approx 6.8$) that is lower than that of the free BA.[43,44] Thus, all four species are in equilibrium leading to a net charge on the complexed or noncomplexed BA species depending on the pH (see figure 5). In order for the sensor to detect the binding of glucose, there should be some difference in the net charge before and after binding. From Figure 5, it is clear that this can be achieved if we convert from **1** to **3** (cyan circles) during the binding process. Compound **1** has the least charge before binding and **3** has a high negative charge after binding. On the basis of this, the optimal working pH would be the one that has a value between pK_{a1} and pK_{a2}. Due to this reason, we choose a working pH of 8.4. At this pH (marked by the vertical line), the relative charge on the complexed species is maximized with respect to the charge on the unbound species. In other words, at this pH, **1** and **3** are expected to be the dominant species before and after complexation respectively. As a result, the net charge on the surface of the CNT is relatively higher in the presence of glucose in comparison to the situation without glucose. It is noteworthy mentioning here that the exact values of pK_{a1} and

(41) Maidan, R.; Heller, A. *J. Am. Chem. Soc.* **1991**, *113*, 9003–9004.
(42) Wang, W.; Gao, X.; Wang, B. *Curr. Org. Chem.* **2002**, *6*, 1285–1317.

(43) Yoon, J.; Czarnik, A. W. *J. Am. Chem. Soc.* **1992**, *114*, 5874–5875.
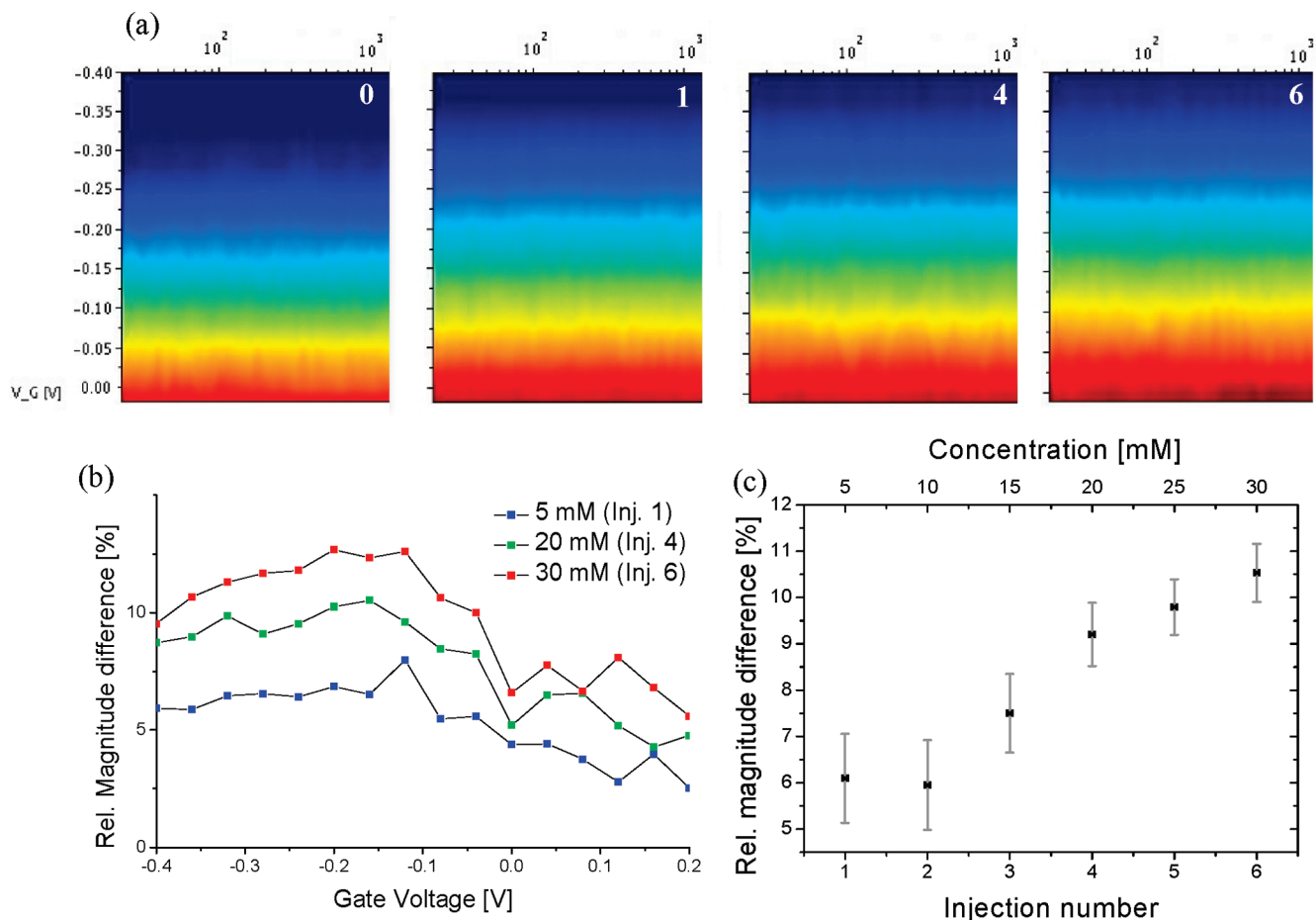(44) Springsteen, G.; Wang, B. *Tetrahedron* **2002**, *58*, 5291–5300.

Figure 4. Concentration dependence of the covalent-BA-CNT-sensors. (a) Z-maps in the absence of glucose (**0**) and after **1**, **4**, and **6** injections of 5 mM glucose. X-axis is frequency in Hz, Y-axis is liquid gate voltage in V. *Scale:* $20-40$ kΩ. Every injection comprises of a 1 μL aliquot of 5 mM glucose followed by a 9 μL aliquot of buffer solution, at which point the impedance response is acquired. (b) The plot shows the relative % change in the magnitude of impedance (averaged in a frequency range of 20 to 500 Hz) for various (1, 4, 6) glucose injections. The relative % change is calculated as $100*(Z^{i}_{glc} - Z_0)/Z_0$ at every gate voltage, where Z_0 is the initial impedance and Z^{i}_{glc} the impedance after the i-th injection of a glucose aliquot. (c) Calibration curve plotting the relative % change as a function of glucose exposure showing a clear concentration dependence. The actual amount of glucose can be read from the top Y-axis.

Table 1. Performance Characteristics of the Non-Enzymatic Single-Wall Carbon Nanotube Sensor for Glucose

Limit of Detection	5 mM
Sensitivity	5 nA/mM @ 80 kΩ
Linear range	$10-20$ mM
Response time	2 minutes

^{a} It is worth mentioning here that these parameters have been attained without any optimization. The parameters must be taken in the sense of a proof-of-concept for the functioning of the glucose sensor. The response time has been extracted from a series of real-time data such as the ones shown in figure S5.

Figure 5. Charge distribution on the surface of BA-functionalized CNTs calculated using the Henderson–Hasselbach relationship. The black curve corresponds to the case without glucose, while the red curve represents the situation with glucose. ($pK_{a1} \approx 8.8$, $pK_{a2} \approx 6.8$). The cyan-colored vertical line corresponds to the working pH of 8.4. Refer to text for further details.

pK_{a2} of the BA-CNT assembly might be slightly different from the known values. However, this would only shift the black and red curves slightly reducing the difference in the net charge by a small amount. On the basis of this picture, we conclude that the increased charge on the covalently attached BA centers in the presence of glucose leads to a stronger scattering of charge carriers resulting in a higher resistance.

While the consistent increase in resistance for a broad gate voltage range and its clear concentration dependence strongly support t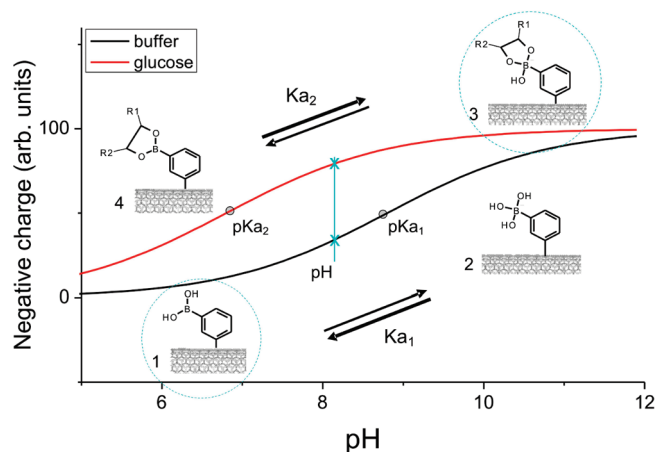he scattering mechanism, two other mechanisms also deserve attention as has been postulated for semiconducting CNTs.[45,46] The first one concerns an alternative effect of the analyte dependent change in charge on the nanotube surface
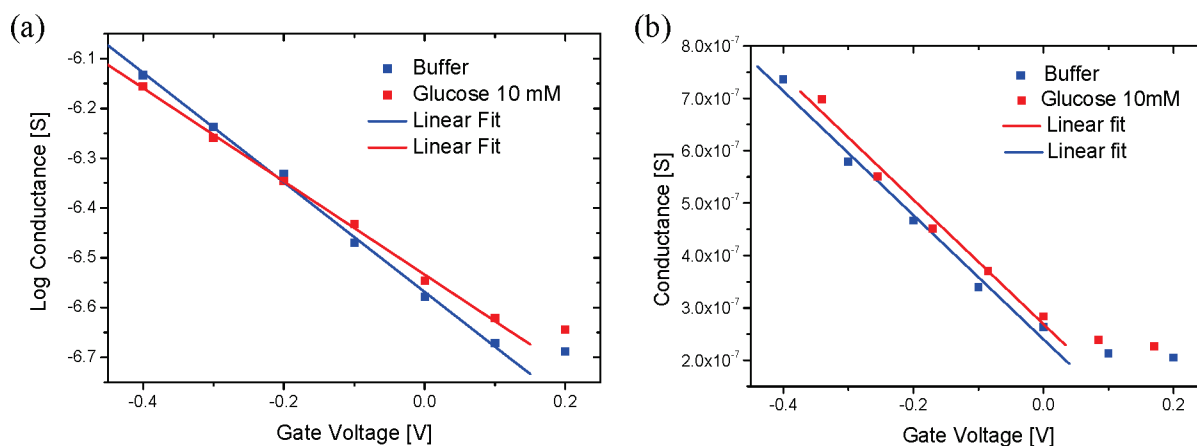
Figure 6. Sensor response for noncovalent-BA-CNT devices showing the gate dependence of the magnitude of impedance at low frequencies. (a) Coupling efficiency (characterized by the slope of transconductance) of the sensor before and after exposure to a 10 mM glucose solution (b) Threshold voltage calculation after correction of the coupling efficiency. In part (a), it can be seen that in the presence of glucose the coupling (slope) is lower, whereas in (b) the binding of glucose to BA moieties shifts the threshold voltage to more positive values.

namely a threshold voltage shift, analogous to the working principle of an ion-selective field-effect transistor (ISFET).[47] In a second scenario, the docking of analytes on the nanotube surface could lead to an increased screening of the gate potential by an increase in the thickness or a change in dielectric constant of the receptor coating. This would alter the effective gate capacitance, which would result in a change in the slope of transconductance characteristics, signifying a modulation of the gate coupling coefficient.

In order to evaluate the presence of the two latter scenarios, it is important to ensure that the attached BA receptors do not alter the electronic structure of the underlying tube. This can be attained if the BA receptors are attached to the CNT surface in a *noncovalent* manner. In addition, it would be important to have a receptor layer thick enough to observe the changes in the electrical characteristics. The electrochemical functionalization provides us with the versatility to achieve both these goals. Through electropolymerization[37] phenyl boronic acid moieties were attached in a noncovalent manner to obtain coatings of a 1 to 3 nm thickness. Figure 6(a),(b) shows the gate response of a typical noncovalently functionalized BA-CNT device in buffer and in a 10 mM glucose solution. It is apparent that the behavior in glucose is quite different from that of the covalent-BA-CNT case, with the device having a higher resistance at negative gate voltage and a lower resistance at positive gate voltage and thus a markedly different slope (see Figure 6(a)). The reduction in slope signifies a less efficient coupling of the liquid gate. Consistent with the above discussion, we attribute this to increased dielectric shielding arising from bound glucose moieties on the BA layer.

Furthermore, at our working pH of 8.4, the bound sugar moieties on the thick BA layer must have an average net charge higher than in the free BA condition, as discussed in Figure 5. That this is indeed the case can be inferred from the curve shown in Figure 6b, where a clear threshold shift can be extracted. The threshold voltage shifts to more positive voltages consistent with the higher negative charge expected on the glucose-BA

complex. For the sample in Figure 6, we calculate this shift to be around 24 mV. Similar values (in the range of a 10−30 mV) have been obtained on other devices. All our measured devices show threshold voltage shifts to more positive voltages and reduced gate coupling in the presence of glucose.

It could be argued that the sensor responses for the covalent case could also be explained using these two mechanisms similar to the noncovalent scenario. However, there are a number of arguments that speak against this possibility. First, the moieties that are covalently attached are very few (submonolayer coverage, as explained before) and hence the screening effect, if present, is expected to be very minimal. Furthermore, since we have more than one tube across the electrodes, it is unlikely that the sparsely distributed charge centers can bring in a significant threshold voltage shift in the gate characteristics. Finally, the gate dependence of resistance in the presence of glucose shows an increase in resistance for all gate voltages in a number of covalent-BA-CNT samples, strongly supporting the previous arguments. Due to these aspects, we conclude that the scattering mechanism plays a dominant role in the sensing response of the covalently coupled BA-CNT devices.

CONCLUSIONS

We have demonstrated a novel type of nonenzymatic sugar sensor based on carbon nanotube devices site-selectively positioned in microfluidic channels. In particular, we have shown that our electrochemical functionalization strategy makes it possible to unravel the subtle mechanisms of transduction of CNT-based sensors. By a careful control of the kind of coupling between the receptor and the nanotube, we could elaborate on the various transduction mechanisms with the help of our impedance detection technique. The sensitivity can be further increased by the use of appropriate receptors that provide a higher binding constant for glucose.[30] These sensors are compact and durable and show promise for applications such as in vivo glucose monitoring. Due to the site-specific functionalization strategy, it is foreseeable that several such sensors be introduced in the same microfluidic channel each designed to detect a specific analyte. The ability to do so will pave the way for lab-on-a-chip systems that can be tailored for specific applications in point-of-care diagnostics.

(45) Back, J. H.; Shim, M. *J. Phys. Chem. B* **2006**, *110*, 23736–23741.
(46) Heller, I.; Janssens, A. M.; Mannik, J.; Minot, E. D.; Lemay, S. G.; Dekker, C. *Nano Lett.* **2008**, *8*, 591–595.
(47) Bergveld, P. *Sens. Actuators B* **2003**, *88*, 1–20.

SUPPORTING INFORMATION AVAILABLE

Confirmation of covalent attachment of BA moieties, reversibility of glucose complexation to BA groups on the CNT surface, control experiments with unmodified CNTs, reversible sensor response to fructose, and real-time data showing the response time and stability against the interferent acetaminophen. This material is available free of charge via the Internet at http://pubs.acs.org.